Journal of Materials Chemistry A

Accepted Manuscript

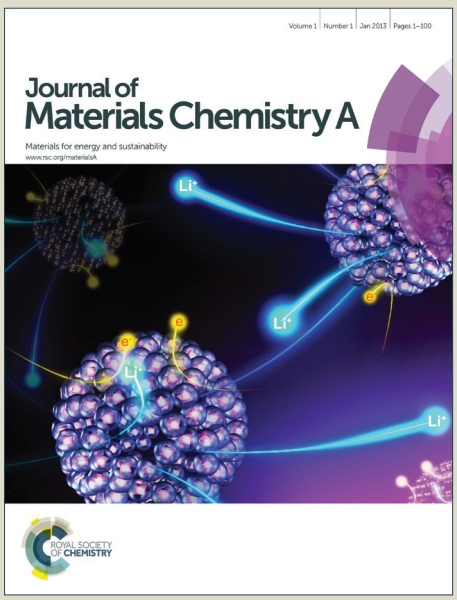

ROYAL SOCIETY OF CHEMISTRY

www.rsc.org/materialsA

Cite this: DOI: 10.1039/c0xx00000x

www.rsc.org/xxxxxx

ARTICLE TYPE

Control of Porosity of Novel Carbazole-modified Polytriazine Frameworks for Highly Selective Separation of CO_2/N_2

Yao Liu,[a] Shaofei Wu,[a] Gang Wang,[a] Guipeng Yu,*[a] Jianguo Guan,[b] Chunyue Pan*[a] and Zhonggang Wang*[c]

Received (in XXX, XXX) Xth XXXXXXXXX 20XX, Accepted Xth XXXXXXXXX 20XX
DOI: 10.1039/b000000x

Engineering porosity and surface functionalization in nanoporous organic polymers remain challenging. Here we achieve the control over the porosity as well as the pre-functionalization of pore walls of a carbazole-modified polytriazine framework by the introduction of three different appended functional groups (methyl, ethyl acetate and phenyl). All the synthesized nanoporous organic polytriazines (NOPs) display good thermal stability, high BET surface areas. The phenyl-anchored framework (NOP-21) exhibits the highest CO_2 capacity (12.3 wt% at 273 K/1 bar) and isoteric heats value (Q_{st}, 37kJ/mol). Besides, the highest selectivity based on ideal adsorbed solution theory (IAST) model at 273K was amazingly observed for the ethyl acetate-appended framework (NOP-20): CO_2/N_2 81 (273K, 1.0 bar), because of uniform ultramicropores through pore engineering. These results suggest a good feasibility for constructing high performance organic porous CO_2 sorbents by controlling porosity.

Introduction

Carbon capture and storage (CCS), which has been widely regarded as one of the most challenges in the 21 century, has become a political and technological priority.[1] Up to now, absorption by monoethanol amine solution is the most widely adopted method for its uniqueness toward CO_2 due to chemical bonding force.[1a,2] However, it suffers from considerable energy penalty required for the CO_2 release for sequestration and regeneration of the amine solution.[3] A promising alternative is porous solid due to its vander wals interaction between sorbent and guest along with low energy requirements.[4]

Various porous adsorbents have been considered for CO_2 separation and capture, including metal-organic frameworks (MOFs), activated carbons, microporous zeolites and nanoporous organic polymers (NOPs).[4b,5] MOFs which have been widely studied due to their extremely high surface areas, typically display a very high capacity to adsorb CO_2 at high pressures (10-50 bar).[4b,6] As a new emerging solid sorbent, NOPs hold the greatest potential for commercial use due to their tailored pore size, low cost, high porosity, and superior thermal/chemical stabilities.[7] Currently, PPN-4[8] presents an impressive CO_2 capacity of 1710 mg/g at 50 bar and 298K which is slightly less than the reported uptake of MOFs to date (1760 mg/g for MIL-101 (Cr) at 50 bar,[9] 2043 mg/g for MOF-210 at 55 bar[10] and 2043 mg/g for NU-100 at 40 bar).[11] The incredible uptake capacity for porous benzimidazole-linked polymers BILP-4 is up to 23.5 wt% under the atmospheric pressure and 273 K,[12] and this value is notably higher than MOFs and zeolites at the same condition.[4b,13] Noted that perfluorinated covalent triazine-based framework FCTF-1-600 represents the highest CO_2 capacity of 24.3 wt% at 1bar and 273K reported for any porous organic polymer-based sorbents under the same conditions.[14] There are, however, only a few porous organic frameworks that simultaneously exhibit significant CO_2 uptake and CO_2-over-N_2 selectivity at the pressures and temperatures relevant for post-combustion capture of CO_2.[15] Therefore, the design and synthesis of porous organic frameworks with high CO_2 uptake and selectivity under ambient conditions remain ongoing challenges.[16] To our best knowledge, a successful adsorbent for CCS means suitable interactions of guest molecules with the adsorbent walls which point the isosteric heat of adsorption (Q_{st}), along with high CO_2/N_2 selectivity.[17] Several factors should be taken into account for a high performance CO_2 sorbent. Firstly, the acceptable binding energy between host and guest CO_2 molecule should enable a strong but reversible adsorption–desorption.[18] Typically, the

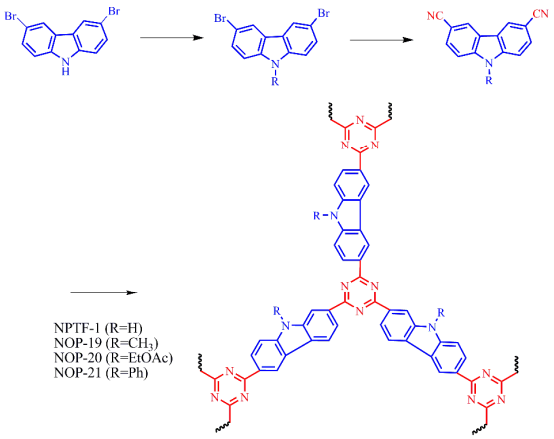

Scheme 1 Schematic representation of the synthesis of NOPs

incorporation of nitrogen-rich polar moieties (such as triazine, and carbazole) into porous frameworks which endow them with strong affinity can improve isosteric heat between the framework and guest molecule by significantly promoted dipole-quadrupole interaction.[19] Secondly, studies have shown that only pores smaller than 1 nm are effective towards CO_2 capture at atmospheric pressure.[20] It seems even more difficult to achieve polymer solids with regular ultramicroporous structure besides the obstacles associated with the introduction of polar surface functionality areas.[21]

9-H-carbazole known for its good electro-activity, is an attractive molecular building block for the construction of nanoporous organic polymers possessing special functions and properties due to the advantages of nitrogen abundance, low cost and facility to tailor-made functionalities.[16,19b,d,22] A typical example is microporous polycarbazole CPOP-1 which presents an extremely high CO_2 uptake (21.2 wt%) and selectivity (25).[19b] Our previous study showed that NPTF-1 modified by carbazole also displayed a comparable capacity and a high selectivity (45).[23] In this paper, carbazole was chosen as a starting monomer and by applying the ionothermal method, a series of nanoporous organic polytriazines (NOPs) containing carbazole-moieties and different functional appended groups were synthesized successfully. To maintain a balance between maximizing the CO_2 uptake and achieving high selectivity for polar NOP adsorbents, we chose functional groups such as methyl, ethyl acetate and phenyl to fulfil controlling the porosity. It contains two aspects: (i) tailoring pore size to obtain polymer solids with uniform micropores; (ii) optimizing surface polarity to achieve sorbents that interact moderately with CO_2 molecules.

Experimental Section

General synthesis procedure for NOPs.

NOP-19. NOP-19 was synthesized by heating a mixture of the 3,6-dibromo-9-methylcarbazole (1.0 g, 4.3 mmol) and $ZnCl_2$ (5.9 g, 43 mmol) in a quartz tube (3 × 10 cm).[23] The tube was evacuated to a high vacuum, and then sealed rapidly. Followed by a temperature program (250°C/10h, 300°C/10h, 350°C/10h, 400°C/20h), the quartz tube was cooled to room temperature, and the reaction mixture was ground and then washed thoroughly with water to remove most of the catalyst. The crude product was stirred in diluted HCl for 15 h to remove the residual salt. The resulting black powder was filtered, and washed successively with water and methyl alcohol, followed by Soxhlet extraction overnight using acetone, methyl alcohol and hexane as eluting solvent sequentially, and dried in vacuum at 150 °C. Yield: 93%

NOP-20. The synthesis method of NOP-20 was almost the same as for NOP-19, and a black solid was obtained starting from ethyl-2-(3,6-dicyano-9H-carbazol-9-yl)acetate. Yield: 90%.

NOP-21. The synthesis method of NOP-21 was almost the same as for NOP-19, and a black solid was obtained starting from 3,6-dicyano-9-phenylcarbazole. Yield: 94%

Result and discussion

Synthesis routes for the three aromatic cyanide monomers with carbazole moieties are outlined in Scheme S1 (ESI†). The starting compound 3,6-dibromo-9H-carbazole was electrophilically substituted in position of 9H by methyl, ethyl acetate and phenyl, respectively, and then the obtained intermediates reacted with CuCN to readily give the precursors. Followed by trimerization of aromatic nitriles, NOP-19, NOP-20 and NOP-21 were coincidently obtained as black monolithic materials in almost quantitative yields (Scheme 1). The chemical structure of the aromatic dinitriles was confirmed by FTIR, ^{1}H NMR as well as GC-TOF/MS (Fig.S1-S9, ESI†). All obtained polymer networks are insoluble in boiled water as well as common organic solvents such as hexane, methanol, acetone, chloroform, THF and DMF, indicating their good chemical stability. The polymerization reaction for NOP-19~21 can be monitored by FTIR spectroscopy (Fig.S1-S3, ESI†). The almost disappearance in the intense C≡N band around 2238 cm^{-1} along with the emergence of strong triazine absorption bands around 1477 (C=N), 1350 (C-N) and 800 cm^{-1} suggest a high degree of crosslinking. Elemental analysis (Tab.S1, ESI†) gives a much lower nitrogen content and concomitantly a much higher C/N ratio than the theoretically calculated values. This indicates that the part of the nitrogen has been lost during the polymerization due to decomposition (Scheme S2, ESI†). Thus, a significant amount of nitriles cleavage of the weakest Ar-CN bonds has to be taken into account.[24b,25] Concerning thermal stability of the obtained frameworks, thermogravimetric analysis (TGA) (Fig.S10, ESI†) shows that the decomposition starts at a temperature of 450 °C under the air atmosphere, suggesting a good thermal stability. To specific up, NOP-20 starts to degrade under 180 °C, which should be attributed to the partial decomposition of ethyl acetate groups. The framework body parts rapidly degrade under extremely high temperatures of around 500 °C, and then the TGA curve settles down steadily, and reveals approximately 4.9 wt% residual $ZnCl_2$.

Morphologies are evaluated by scanning electron microscopy (SEM, Fig.S11-S13, ESI†). All the polymer samples are aggregates of uniform and compact microgel particles of the size of 100-200 nm. Additionally, the microstructure was studied by high-resolution transmission electron microscopy (HR-TEM) and powder X-ray diffraction (PXRD). Alternately, a dark and bright area can be clearly observed from HR-TEM images (Fig.S14-S16, ESI†), implying a porous structure. The powder X-ray diffraction spectrums (Fig.S17-S19, ESI†) are featureless indicating an amorphous nature. Pore structure of the resultant networks was

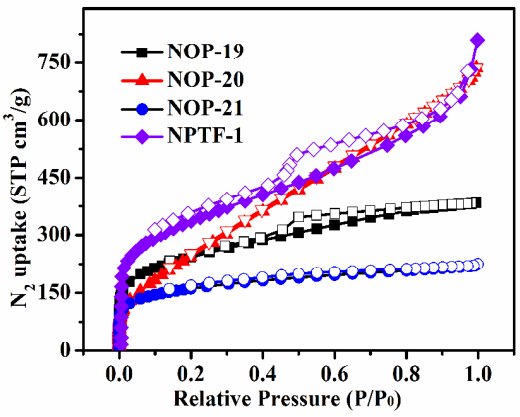

Fig.1 N_2 sorption isotherms of NOPs at 77 K

explored by nitrogen sorption experiments at 77 K after fully out-gassed at 200°C for 12 h. As shown in Fig.1, similar to NPTF-1, NOP-19~21 exhibit a sharp uptake in the low pressure region (P/P_0<0.001), implying a microporous property, and another relative steady rise phase range from 0.2 to 0.8 corresponding to the presence of mesopores.[26] However, not surprisingly, the sorption isotherms of NOPs modified by different side-groups demonstrate great changes relative to NPTF-1. As depicted, the isotherms for NOP-20 and NOP-21 are almost completely reversible, while the sorption isotherm of NOP-19 modified by methyl group exhibits a hysteresis loop which can attributed to the softness of organic polymer skeleton and swelling effect in critical nitrogen. NOP-20 shows an significant increase of nitrogen uptake over 0.8 (P/P_0), suggesting the presence of macroporous structure which can be interpreted as the inter-particulate voids arising from the loose packing of small particles as observed in the SEM micrographs.[27] According to IUPAC, the isotherms for NOP-19 and NOP-21 could be classified as Type IV isotherm which suggest the obtaind frameworks are microporous materials with supererogatory mesoporosity. The isotherm for NOP-20 presents small degree of hysteresis upon desorption, implying that the isotherm is Type I with some Type IV characteristics which account for relatively mesoporous dominating this material. The apparent surface areas calculated from Brunauer-Emmett-Teller (BET) models for relative pressure between 0.01 and 0.1 were shown in Table 1. The determined BET surface areas of NOPs decrease with the increasing size of the appended groups. NOP-19 has the highest surface area of 982 m^2/g, followed by 952 m^2/g for NOP-20 and 565 m^2/g for NOP-21.

Pore size distribution was estimated by fitting the nitrogen uptake branch of the isotherms with Non-local density functional theory (NLDFT), indicating that a significant fraction of the pore surface still originates from micropores with a diameter less than 20 Å (Fig. 2). NOP-20 has a relatively broad distribution ranging from 4.0 Å to 100 Å, while the dominating pore size distribution extends from 20 Å to 70 Å. This is consistent with the description of the nitrogen adsorption and desorption isotherm. One reason should be taken into account for this broad distribution. Ethyl acetate group decomposes partly due to its poor stability under high temperature, and hence the leaving organic units can act as an additional template, which enhances the pore size. The occurrence of ultramicropores (<5 Å) in NOP-20 supported our idea that the release of decomposition organic units from the framework possibly accounts for the generation of extra micropores in NOP-20. Careful examination of NOP-21 shows its narrowest distribution, mainly locating at 5.6 Å along with a small proportion of micropores of 13 Å. This is in good accordance with our idea that replacing H atoms with phenyl group would reduce the effective pore size of NPTF-1. From the three distribution curves, we have recognized the similarities of three locations, 27 Å and 34 Å for mesopores and 13 Å for micropores, indicative of similar topology structures even after the structural modification. To be sure, substituting methyl, ethyl acetate and phenyl groups for H atoms tailored the pore size distribution as we expected. Pore size distribution can be confirmed by the level of microporosity which is described by the ratio of micropore to total pore volume ($V_{0.1}/V_{tot}$) (Table 1).

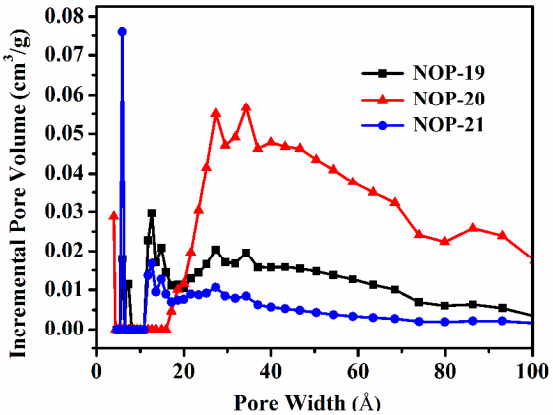

Fig. 2 NL-DFT pore size distribution curves of NOPs

Micropore volume (total pore volume) was calculated from single-point measurements at 0.1 (0.9) bar and detected to be 0.33 (0.58), 0.28 (1.00), and 0.22 (0.33) cm^3/g for NOP-19, NOP-20, and NOP-21, respectively. The total pore volumes basically follow the order of the volume of appended functional groups: NOP-20 (1.00 cm^3/g) > NPTF-1 (0.93 cm^3/g) > NOP-19 (0.58 cm^3/g) > NOP-21 (0.33 cm^3/g). This observation acts in accordance with previous reports on the fact that pore volumes of the networks become smaller when the functional side-groups in the pore surface are getting huger.[14,28] The only exception is that NOP-20 functionalized by ethyl acetate demonstrates a higher total pore volume than NPTF-1, possibly because of the broad distribution caused by the partial decomposition of ethyl acetate groups under high temperature. Notably, NOP-21 has the lowest total pore volume of 0.33 cm^3/g, while the $V_{0.1}/V_{tot}$ was the highest of 70% (57% and 28% for NOP-19 and NOP-20). In this case, we consider that the high micropore content of NOP-21 accounts for the introduction of phenyl that occupying the effective pore volume.

CO_2 adsorption isotherms of the porous networks at 273 and 298 K (Fig. 3) demonstrated that the absorbed CO_2 amount continually increased with the pressure, implying that the adsorption has not reached its equilibrium or saturated state in the investigated pressure range.[29] Among the obtained three porous frameworks, NOP-21 with pendant phenyl unit exhibits the highest CO_2 uptake of 123 mg/g at 273 K (69 mg/g at 298 K). The corresponding values for NOP-20 are slightly lower of 118 mg/g (72 mg/g at 298 K), while NOP-19 with methyl group displays a capacity of 106 mg/g (69 mg/g at 298 K), which is also comparably much higher than those obtained values of N_2 isotherms. It is noted that the highest CO_2 uptake capacity is attained by NOP-21 with the lowest S_{BET}. Only pores less than 1.0 nm are proved to be effective towards CO_2 capture at low pressure since the molecular size of CO_2 is 0.36 nm.[20] Another possibility can be attributed to the measurement in which we utilize the critical nitrogen adsorption-desorption isotherm to calculate the BET and porosity. It is generally known that the resolving power of nitrogen molecules for micropores is not enough. In reality, it is more appropriate to investigate adsorption properties for microporous materials, particularly those with ultramicropores, using CO_2 probe at 195 K rather than N_2 at 77 K.[30] Therefore, the actual BET surface area of NOP-21

Table 1 The properties of porosity, gas uptake and isosteric heat of adsorption of NOPs

Sample	S_{BET} [a] (m^2/g)	$V_{0.1}$ [b] (cm^3/g)	V_{tot} [c] (cm^3/g)	$V_{0.1}/V_{tot}$	CO_2 Uptake 273 K (wt%)	Q_{st} for CO_2 (kJ/mol)
NOP-19	982	0.33	0.58	57%	10.6	28
NOP-20	952	0.28	1.00	28%	11.8	32
NOP-21	565	0.22	0.33	70%	12.3	37
NPTF-1	1187	0.44	0.93	47%	13.2	34

[a] Brunauer- Emmett-Teller surface area. [b] Pore volume determined from the N_2 isotherm at P/P_0= 0.1. [c] Total pore volume determined from the N_2 isotherm at P/P_0=0.9.

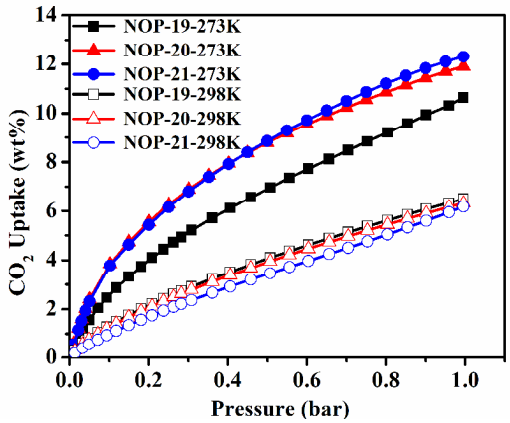

Fig. 3 CO_2 sorption isotherms of NOPs at 273 K and 298K

contributed by the microporous part may be much higher than the measured value, which is in good accordance with its high CO_2 adsorption capacity. No matter what kind of explanation we adopt, the high micropore content of NOP-21 should be the decisive factor for its high load. The adsorption quantity of NOP-19 is lower than that of NOP-21 by about 20 mg/g in spite of a double BET. It can be boiled down to the broad distribution and the slight polarity changes by the introduction of methyl group. Compared with NOP-19, the good capacity for NOP-20 can be attributed to a good balance between the enhanced polarity by the introduction of ethyl acetate which promotes the interaction of host-gas guest, and the hierarchical pores with broad distribution ranging from 4.0 Å to 80 Å. It should be noted that the overall CO_2 adsorption capacities of NOP-19~21 are not greatly enhanced, on the contrary the uptake is decreased by 7~20mg/g relative to the unmodified sample (NPTF-1). This phenomenon can be interpreted as the decreased BET surface areas and weakened pore surface polarity with the replacement of N-H bond by *N*-methyl, *N*-ethyl acetate and *N*-phenyl. In general, the CO_2 capacity for NOPs notably exceeds a lot of organic porous networks, namely PAF-3 (80 mg/g at 273K),[31] CMP-1 (90 mg/g at 273K),[32] TBI-2 (118 mg/g at 273K),[33] A-B2^{III} (119 mg/g at 273K),[30c] but is inferior to materials such as FCTF-1-600 (243 mg/g at 273K),[14] BILP-4 (235 mg/g at 273K),[12] and CPOP-1 (212 mg/g at 273K).[19b]

To gain further insights of CO_2 adsorption, Q_{st} (CO_2 isoteric heats) were obtained using Clausius-Clapeyron equation and Viral equation from their CO_2 adsorption date collected at 273 and 298 K (Fig. 4). The Q_{st} value at the initial adsorption stage (low gas loading) mainly reflects the interaction strength between CO_2 and the sorbent. As shown in Fig. 4, the Q_{st} values at a low adsorption amount are arranged in the following order: NOP-21 (37 kJ/mol)> NOP-20 (32 kJ/mol)> NOP-19 (28 kJ/mol). This is consistent with the trend of the CO_2 capacity values at 273K at 1bar. NOP-21 has the highest Q_{st} value owing to its large content of micropores. NOP-20 has considerable higher Q_{st} values than NOP-19 over a wide range of gas loadings, suggesting that the incorporation of polar group into the framework indeed enhances its affinity towards CO_2. All three materials show remarkable high Q_{st} values for CO_2 (>28 kJ/mol) which are higher than many known porous polymers such as ZTF-1 (25.4 kJ mol),[34] HCP-1 (23.5 kJ mol),[20a] BILPs (26.7-28.8 kJ mol).[7a,12,35] These values are also comparable to many attracting porous solids, namely CMP-1-COOH (33 kJ/mol),[28] MOPs-C (34 kJ/mol),[16] PI-1 (34 kJ/mol)[36] and FCTF-1 (35 kJ/mol).[14] This may be reasonable considering the fact that the triazine-based frameworks with abundant nitrogen content intrinsically favor CO_2 adsorption through electrostatic interaction.[14,37]

Flue gas from coal-fired power plants contains ~15% CO_2 at a pressure about 1 bar, and hence the CO_2 uptake capacity at 0.15 bar and the N_2 adsorption at 0.85 bar are important factors for practical applications. NOP-21 has a CO_2 uptake of 24.5 cm^3/g at 0.15 bar and 273K. This value is higher than those of many other polymer networks and can be comparable to A-B1^{III} (26.9 cm3/g at 273K),[30c] PCTFs,[38] and BILPs (28.1-44.6 cm3/g at 273K),[12] but still less than some impressive porous solids such as FCTF-1 (39.4 cm^3/g at 0.1bar at 273K),[14] PPN-6-CH2-DETA (68.1 cm^3/g at 295K)[35] and MgMOF-74 (112 cm^3/g at 293K).[36] This indicates that CO_2 could be kinetically replaced by N_2 on adsorption in such a adsorbent.[30c] Evaluation of the selectivity of adsorbents under atmospheric pressure for CO_2-N_2 mixture was essential for realistic post-combustion capture of CO_2 (total carbon dioxide

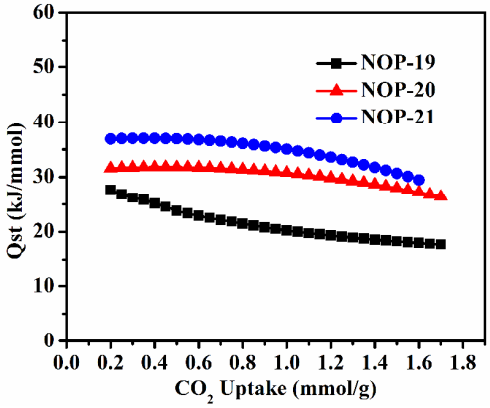

Fig. 4 Plots of the isosteric heat of adsorption (Q_{st}) for CO_2 of NOPs versus CO_2 uptake

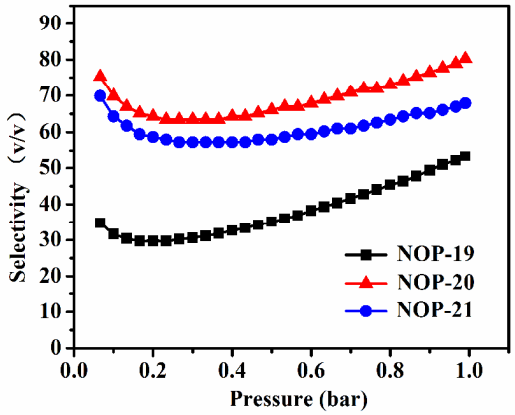

Fig. 5 IAST selectivities of CO_2 over N_2 for binary gas mixtures of 15/85 molar composition in NOPs at 273 K

Table 2 Summary of the CO_2/N_2 selectivity for NOPs

Sample	273K $S^a_{(CO2/N2)}$	273K $S^b_{(CO2/N2)}$	273K $S^c_{(CO2/N2)}$
NOP-19	53	35	24
NOP-20	81	44	71
NOP-21	68	42	64

[a] $S^a_{(CO_2/N_2)}$ is calculated by the IAST model from 85% N_2 and 15% CO_2, 1 bar. [b] $S^b_{(CO_2/N_2)}$ is calculated by dividing the mass of CO_2 taken up at 0.15 bar by that of N_2 taken up at 0.85 bar. [c] $S^c_{(CO_2/N_2)}$ is calculated from initial slope calculations at 273K.

content <15%, 1bar). Ideal adsorbed solution theory (IAST) model has been documented to accurately predict binary gas mixture adsorption in many porous materials. The dual-site Langmuir-Freundlich equation is used to fit the experimental single component adsorption isotherm, and the IAST model were adoped to imitate selectivity of CO_2 over N_2 at an equilibrium partial pressure of 0.85 bar (N_2) and 0.15 bar (CO_2) in the bulk phase (Fig. S20-S22, ESI†).[39] Notably, NOP-19 ~NOP-21 exhibit pronounced CO_2 uptake and fairly low N_2 adsorption at a pressure lower than 1 bar. The different adsorption ability towards CO_2 and N_2 provides a basis for the selective capture of CO_2 from gas mixture streams. As expected, NOPs demonstrate much higher CO_2-over-N_2 selectivity than NPTF-1 (45). Among the three polymers, NOP-20 has the highest CO_2-over-N_2 selectivity of 81 (Fig.5) despite its smaller CO_2 uptake compared to NOP-21, which may be ascribed to a larger proportion of ultramicropores relative to the others.[7b,40] Compared to NOP-19, 21, NOP-20 has a broad pore size distribution ranging from 4.0 Å to 100 Å, while the dominating pore size distribution extends from 20 Å to 70 Å. The occurrence of ultramicropores (<5 Å) in NOP-20 may be essential to this high selectivity. Since such ultramicropores have pore sizes (0.40 nm) approaching the diameter of N_2 molecules (0.364 nm), they could offer mark kinetic selectivity in separation of CO_2 from N_2. Therefore, it may be resonable that NOP-20 processes the lowest N_2 capacity at 273K and 1 bar (0.080, 0.072, and 0.098 cm^3/g for NOP-19, NOP-20, and NOP-21, respectively). NOP-19 and NOP-21 exhibit good selectivities ranging from 53 to 68, depending on the size of the pendant groups. Although the selectivity parameters are a little lower than some known porous solids such as PPN-6-CH_2-DETA (442),[39c] CuBTTri (329)[41] and BILP-2 (113),[12] they do exceed those of most MOFs,[42] ZIFs,[43] cage molecules[44] and porous organic frameworks.[19e]

Additionally, selectivity was calculated by the mass of CO_2 taken up at 0.15 bar divided by the mass of N_2 taken up at 0.85 bar.[17b,45] As shown in Table 2 (Fig.S23-S25 ESI†), NOP-19, 20, 21 demonstrate CO_2/N_2 selectivities of 35, 44, and 42, respectively. Furthermore, the CO_2/N_2 selectivity was also calculated by using the ratios of Henry's law constants. According to initial slope calculations of pure gas isotherms (Fig.S26-S28, ESI†) presented in Table 2, similar trend of the CO_2/N_2 selectivity levels is observed. Nevertheless, the CO_2/N_2 selectivities obtained from the three methods are still in reasonable agreement. Due to their high heats of adsorption and selectivity of CO_2-over-N_2, the synthesized NOPs have good potential for post-combustion CO_2 capture.

Conclusions

Based on NPTF-1, substituting methyl, ethyl acetate and phenyl groups for H atoms optimized the surface functionality and the pore size simultaneously, leading to three new sorbents. Their chemical structure was confirmed by FTIR, solid-state ^{13}C CP/MAS NMR spectra, and elemental analyses. The analysis of N_2 sorption isotherms reveals that three functional polymers have quite different pore size distributions. Within these frameworks, NOP-21 possesses the highest CO_2 (12.3 wt% at 273 K and 1bar) uptake due to a more uniform and smaller pore size distribution, and NOP-20 displays the best CO_2/N_2 ideal selectivity of 81 (273 K) due to a larger proportion of uniform ultramicropores. The above results indicate that it is a facile approach to engineer the porosity (pore size) and surface polarity. The resulted polymers are promising candidates as adsorbents for CO_2 capture in the environment and energy field.

Acknowledgements

We acknowledge the financially support from the National Science Foundation of China (Nos. 21204103 and 21376272), Hunan Provincial Natural Science Foundation of China (13JJ413), China Postdoctoral Science (2012M521535) and State Key Laboratory of Advanced Technology for Materials Synthesis and Processing (2012-KF-14) and State Key Laboratory of Fine Chemicals (KF1206).

Notes and references

[a] *Key Laboratory of Resources Chemistry of Nonferrous Metals Ministry of Education, College of Chemistry and Chemical Engineering , Central South University, Changsha 410083, China. E-mail:gilbertyu@csu.edu.cn; panchunyue@sina.com.*
[b] *State Key Laboratory of Advanced Technology For Materials Synthesis and Processing, Wuhan University of Technology, Wuhan 430070, China*
[c] *Department of Polymer Science & Materials, State Key Laboratory of Fine Chemicals, Dalian University of Technology, Dalian 116012, China. E-mail: zgwang@dlut.edu.cn*

†Electronic Supplementary Information (ESI) available: Synthesis and Characterization data. See DOI: 10.1039/b000000x/.

1 (a) R. S. Haszeldine, *Science*, **2009**, 325, 1647-1652; (b) T. C. Drage, C. E. Snape, L. A. Stevens, J. Wood, J. W. Wang, A. I. Cooper, R. Dawson, X. Guo, C. Satterley and R. Irons, *J. Mater. Chem.*, **2012**, *22*, 2815-2823; (c) H. C. Chen, F. G. Sun, J. T. Wang, W. C. Li, W. M. Qiao, L. C. Ling and D. H. Long, *J. Phys. Chem. C*, **2013**, *117*, 8318-8328; (d) B. Y. Li, Y. H. Duan, D. Luebke and B. Morreale, *Appl. Energ.*, **2013**, *102*, 1439-1447.

2 (a) H. Q. Yang, Z. H. Xu, M. H. Fan, R. Gupta, R. B. Slimane, A. E. Bland and I. Wright, *J. Environ. Sci.-China,* **2008**, *20*, 14-27; (b) G. T. Rochelle, *Science,* **2009**, *325*, 1652-1654.

3 (a) A. L. Chaffee, G. P. Knowles, Z. Liang, J. Zhany, P. Xiao and P. A. Webley, *Int. J. Greenh. Gas Con.,* **2007**, *1*, 11-18; (b) D. Aaron and C. Tsouris, *Separ. Sci. Technol.,* **2005**, *40*, 321-348; (c) M. S. Jassim, G. Rochelle, D. Eimer and C. Ramshaw, *Ind. Eng. Chem. Res.,* **2007**, *46*, 2823-2833.

4 (a) M. Z. Jacobson, *Energ. Environ. Sci.,* **2009**, *2*, 148-173; (b) D. M. D'Alessandro, B. Smit and J. R. Long, *Angew. Chem. Int. Ed.,* **2010**, *49*, 6058-6082.

5 (a) R. E. Morris and P. S. Wheatley, *Angew. Chem. Int. Ed.,* **2008**, *47*, 4966-4981; (b) J. Liu, P. K. Thallapally, B. P. McGrail, D. R. Brown and J. Liu, *Chem. Soc. Rev.,* **2012**, *41*, 2308-2322; (c) G. P. Hao, W. C. Li, D. Qian and A. H. Lu, *Adv. Mater.,* **2010**, *22*, 853-857; (d) S. Q. Ma and H. C. Zhou, *Chem. Commun.,* **2010**, *46*, 44-53; (e) R. Thiruvenkatachari, S. Su, H. An and X. X. Yu, *Prog. Energ. Combust.,* **2009**, *35*, 438-455; (f) X. M. Liu, Y. H. Xu, Z. Q. Guo, A. Nagai and D. L. Jiang, *Chem. Commun.,* **2013**, *49*, 3233-3235.

6 (a) G. Ferey, C. Serre, T. Devic, G. Maurin, H. Jobic, P. L. Llewellyn, G. De Weireld, A. Vimont, M. Daturi and J. S. Chang, *Chem. Soc. Rev.,* **2011**, *40*, 550-562; (b) A. R. Millward and O. M. Yaghi, *J. Am. Chem. Soc.,* **2005**, *127*, 17998-17999; (c) H. S. Choi and M. P. Suh, *Angew. Chem. Int. Ed.,* **2009**, *48*, 6865-6869; (d) T. M. McDonald, W. R. Lee, J. A. Mason, B. M. Wiers, C. S. Hong and J. R. Long, *J. Am. Chem. Soc.,* **2012**, *134*, 7056-7065; (e) K. Sumida, D. L. Rogow, J. A. Mason, T. M. McDonald, E. D. Bloch, Z. R. Herm, T. H. Bae and J. R. Long, *Chem. Rev.,* **2012**, *112*, 724-781.

7 (a) M. G. Rabbani, T. E. Reich, R. M. Kassab, K. T. Jackson and H. M. El-Kaderi, *Chem. Commun.,* **2012**, *48*, 1141-1143; (b) Z. H. Xiang, X. Zhou, C. H. Zhou, S. Zhong, X. He, C. P. Qin and D. P. Cao, *J. Mater. Chem.,* **2012**, *22*, 22663-22669; (c) P. Katekomol, J. Roeser, J. Weber and A. Thomas, *Chem. Mater.,* **2013**; (d) P. Katekomol, J. Roeser, M. Bojdys, J. Weber and A. Thomas, *Chem. Mater.,* **2013**, *25*, 1542-1548.

8 W. G. Lu, D. Q. Yuan, D. Zhao, C. I. Schilling, O. Plietzsch, T. Muller, S. Brase, J. Guenther, J. Blumel, R. Krishna, Z. Li and H. C. Zhou, *Chem. Mater.,* **2010**, *22*, 5964-5972.

9 P. L. Llewellyn, S. Bourrelly, C. Serre, A. Vimont, M. Daturi, L. Hamon, G. De Weireld, J. S. Chang, D. Y. Hong, Y. K. Hwang, S. H. Jhung and G. Ferey, *Langmuir,* **2008**, *24*, 7245-7250.

10 H. Furukawa, N. Ko, Y. B. Go, N. Aratani, S. B. Choi, E. Choi, A. O. Yazaydin, R. Q. Snurr, M. O'Keeffe, J. Kim and O. M. Yaghi, *Science,* **2010**, *329*, 424-428.

11 O. K. Farha, A. O. Yazaydin, I. Eryazici, C. D. Malliakas, B. G. Hauser, M. G. Kanatzidis, S. T. Nguyen, R. Q. Snurr and J. T. Hupp, *Nat. Chem.,* **2010**, *2*, 944-948.

12 M. G. Rabbani and H. M. El-Kaderi, *Chem. Mater.,* **2012**, *24*, 1511-1517.

13 Y. E. Cheon and M. P. Suh, *Chem. Commun.,* **2009**, 2296-2298.

14 Y. Zhao, K. X. Yao, B. Teng, T. Zhang and Y. Han, *Energ. Environ. Sci.,* **2013**, *6*, 3684-3692.

15 T. Ben, K. Shi, Y. Cui, C. Y. Pei, Y. Zuo, H. Guo, D. L. Zhang, J. Xu, F. Deng, Z. Q. Tian and S. L. Qiu, *J. Mater. Chem.,* **2011**, *21*, 18208-18214.

16 R. Dawson, E. Stockel, J. R. Holst, D. J. Adams and A. I. Cooper, *Energ. Environ. Sci.,* **2011**, *4*, 4239-4245.

17 (a) J. R. Holst and A. I. Cooper, *Adv Mater* **2010**, *22*, 5212-5216; (b) T. İslamoğlu, M. G. Rabbani and H. M. El-Kaderi, *J. Mater. Chem. A,* **2013**, *1*, 10259-10266.

18 (a) H. A. Patel, S. H. Je, J. Park, D. P. Chen, Y. Jung, C. T. Yavuz and A. Coskun, *Nat. Commun.,* **2013**, *4*; (b) M. Saleh, J. N. Tiwari, K. C. Kemp, M. Yousuf and K. S. Kim, *Environ. Sci. Technol.,* **2013**, *47*, 5467-5473; (c) J. Chun, S. Kang, N. Kang, S. M. Lee, H. J. Kim and S. U. Son, *J .Mater. Chem. A.,* **2013**, *1*, 5517-5523.

19 (a) H. Lim, M. C. Cha and J. Y. Chang, *Macromol. Chem. Phys.,* **2012**, *213*, 1385-1390; (b) Q. Chen, M. Luo, P. Hammershoj, D. Zhou, Y. Han, B. W. Laursen, C. G. Yan and B. H. Han, *J. Am. Chem. Soc.,* **2012**, *134*, 6084-6087; (c) M. J. Bojdys, J. Jeromenok, A. Thomas and M. Antonietti, *Adv. Mater.* **2010**, *22*, 2202-2205; (d) C. Maeda, T. Yoneda, N. Aratani, M. C. Yoon, J. M. Lim, D. Kim, N. Yoshioka and A. Osuka, *Angew. Chem. Int. Ed.,* **2011**, *50*, 5690-5693; (e) Z. H. Xiang and D. P. Cao, *J. Mater. Chem. A,* **2013**, *1*, 2691-2718.

20 (a) C. F. Martin, E. Stockel, R. Clowes, D. J. Adams, A. I. Cooper, J. J. Pis, F. Rubiera and C. Pevida, *J. Mater. Chem.,* **2011**, *21*, 5475-5483; (b) B. Y. Li, R. N. Gong, W. Wang, X. Huang, W. Zhang, H. M. Li, C. X. Hu and B. E. Tan, *Macromolecules,* **2011**, *44*, 2410-2414; (c) D. Cazorla-Amorós, J. Alcaniz-Monge and A. Linares-Solano, *Langmuir,* **1996**, *12*, 2820-2824.

21 (a) P. Kaur, J. T. Hupp and S. T. Nguyen, *ACS Catalysis,* **2011**, *1*, 819-835; (b) D. C. Sherrington, *Chem. Commun.,* **1998**, 2275-2286; (c) N. B. McKeown and P. M. Budd, *Macromolecules,* **2010**, *43*, 5163-5176; (d) G. Li and Z. Wang, *Macromolecules,* **2013**, *46*, 3058-3066.

22 A. P. Katsoulidis, S. M. Dyar, R. Carmieli, C. D. Malliakas, M. R. Wasielewski and M. G. Kanatzidis, *J. Mater. Chem. A.,* **2013**, *1*, 10465-10473.

23 S. F. Wu, Y. Liu, G. P. Yu, J. G. Guan, C. Y. Pan,Y. Du, X. Xiong and Z. G. Wang. 2014, subimited to *Macromolecules*, unpubilished data.

24 (a) P. Kuhn, M. Antonietti and A. Thomas, *Angew. Chem. Int. Ed.,* **2008**, *47*, 3450-3453; (b) A. Bhunia, V. Vasylyeva and C. Janiak, *Chem. Commun.,* **2013**, *49*, 3961-3963.

25 P. Kuhn, A. Forget, D. S. Su, A. Thomas and M. Antonietti, *J. Am. Chem. Soc.,* **2008**, *130*, 13333-13337.

26 (a) F. Rouqueol, J. Roquerol and K. Sing, Adsorption by Powders and Porous Solids, Academic Press, London, **1999**; (b) S. Kandambeth, A. Mallick, B. Lukose, M. V. Mane, T. Heine and R. Banerjee, *J. Am. Chem. Soc.,* **2012**, *134*, 19524-19527.

27 H. Yu, C. Shen, M. Tian, J. Qu, and Z. Wang, *Macromolecules*, **2012**, *45*, 5140-5150

28 R. Dawson, D. J. Adams and A. I. Cooper, *Chem. Sci.,* **2011**, *2*, 1173-1177.

29 Y. Yang, Q. Zhang, S. Zhang and S. Li, *Polymer,* **2013**, *54*, 5698-5702.

30 (a) M. Kanezashi, T. Shioda, T. Gunji and T. Tsuru, *AIChE Journal,* **2012**, *58*, 1733-1743; (b) J. Weber, Q. Su, M. Antonietti and A. Thomas, *Macromol. Rapid. Comm.,* **2007**, *28*, 1871-1876; (c) C. Xu and N. Hedin, *J. Mater. Chem. A,* **2013**, *1*, 3406-3414; (d) H. Y. Zhao, Z. Jin, H. M. Su, J. L. Zhang, X. D. Yao, H. J. Zhao and G. S. Zhu, *Chem. Commun.,* **2013**, *49*, 2780-2782.

31 T. Ben, C. Y. Pei, D. L. Zhang, J. Xu, F. Deng, X. F. Jing and S. L. Qiu, *Energ. Environ. Sci.,* **2011**, *4*, 3991-3999.

32 J. X. Jiang, F. Su, A. Trewin, C. D. Wood, H. Niu, J. T. A. Jones, Y. Z. Khimyak and A. I. Cooper, *J. Am. Chem. Soc.,* **2008**, *130*, 7710-7720.

33 Y. C. Zhao, Q. Y. Cheng, D. Zhou, T. Wang and B. H. Han, *J. Mater. Chem.,* **2012**, *22*, 11509-11514.

34 T. Panda, P. Pachfule, Y. Chen, J. Jiang and R. Banerjee, *Chem. Commun.,* **2011**, *47*, 2011-2013.

35 M. G. Rabbani and H. M. El-Kaderi, *Chem. Mater.,* **2011**, *23*, 1650-1653.

36 A. Laybourn, R. Dawson, R. Clowes, J. A. Iggo, A. I. Cooper, Y. Z. Khimyak and D. J. Adams, *Polym. Chem-Uk,* **2012**, *3*, 533-537.

37 Y. Zhao, L. Zhao, K. X. Yao, Y. Yang, Q. Zhang and Y. Han, *J. Mater. Chem.,* **2012**, *22*, 19726-19731.

38 A. Bhunia, I. Boldog, A. Möller and C. Janiak, *J. Mater. Chem. A,* **2013**, *1*, 14990-14999.

39 (a) T. Ben, Y. Li, L. Zhu, D. Zhang, D. Cao, Z. Xiang, X. Yao and S. Qiu, *Energ. Environ. Sci.,* **2012**, *5*, 8370-8376; (b) W. Lu, D. Yuan, J. Sculley, D. Zhao, R. Krishna and H.-C. Zhou, *J. Am. Chem. Soc.,* **2011**, *133*, 18126-18129; (c) W. G. Lu, J. P. Sculley, D. Q. Yuan, R. Krishna, Z. W. Wei and H. C. Zhou, *Angew. Chem. Int. Ed.,* **2012**, *51*, 7480-7484.

40 Z. Xiang, D. Cao, W. Wang, W. Yang, B. Han and J. Lu, *J. Phys. Chem. C,* **2012**, *116*, 5974-5980.

41 T. M. McDonald, D. M. D'Alessandro, R. Krishna and J. R. Long, *Chem. Sci.,* **2011**, *2*, 2022-2028.

42 (a) J. R. Li, J. Sculley and H. C. Zhou, *Chem. Rev.,* **2012**, *112*, 869-932; (b) J.-R. Li, Y. Ma, M. C. McCarthy, J. Sculley, J. Yu, H.-K.

Jeong, P. B. Balbuena and H.-C. Zhou, *Coord. Chem. Rev.,* **2011**, *255*, 1791-1823.
43 A. Phan, C. J. Doonan, F. J. Uribe-Romo, C. B. Knobler, M. O'Keeffe and O. M. Yaghi, *Accou. Chem. Res.,* **2010**, *43*, 58-67.
44 S. Jiang, J. Bacsa, X. Wu, J. T. Jones, R. Dawson, A. Trewin, D. J. Adams and A. I. Cooper, *Chem. Commun.,* **2011**, *47*, 8919-8921.
45 M. R. Liebl and J. r. Senker, *Chem. Mater.,* **2013**, *25*, 970-980.